JACS
JOURNAL OF THE AMERICAN CHEMICAL SOCIETY

ARTICLE

pubs.acs.org/JACS

Predicting the Size and Properties of Dendrimersomes from the Lamellar Structure of Their Amphiphilic Janus Dendrimers

Mihai Peterca,[†,‡] Virgil Percec,[*,†] Pawaret Leowanawat,[†] and Annabelle Bertin[†]

[†]Roy & Diana Vagelos Laboratories, Department of Chemistry, University of Pennsylvania, Philadelphia, Pennsylvania 19104-6323, United States

[‡]Department of Physics and Astronomy, University of Pennsylvania, Philadelphia, Pennsylvania 19104-6396, United States

Supporting Information

ABSTRACT: Dendrimersomes are stable, monodisperse unilamellar vesicles self-assembled in water from amphiphilic Janus dendrimers. Their size, stability, and membrane structure are determined by the chemical structure of Janus dendrimer and the method of self-assembly. Comparative analysis of the periodic arrays in bulk and dendrimersomes assembled by ethanol injection in water of 11 libraries containing 108 Janus dendrimers is reported. Analysis in bulk and in water was performed by differential scanning calorimetry, X-ray diffraction, dynamic light scattering, and cryo-TEM. An inverse proportionality between size, stability, mechanical properties of dendrimersomes, and thickness of their membrane was discovered. This dependence was explained by the tendency of alkyl chains forming the hydrophobic part of the dendrimersome to produce the same local packing density regardless of the branching pattern from the hydrophobic part of the dendrimer. For the same hydrophobic alkyl chain length, the largest, toughest, and most stable dendrimersomes are those with the thinnest membrane that results from the interdigitation of the alkyl groups of the Janus dendrimer. A simplified spherical-shell model of the dendrimersome was used to demonstrate the direct correlation between the concentration of Janus dendrimer in water, *c*, and the size of self-assembled dendrimersome. This concentration-size dependence demonstrates that the mass of the vesicle membrane is proportional with *c*. A methodology to predict the size of the dendrimersome based on this correlation was developed. This methodology explains the inverse proportionality between the size of dendrimersome and its membrane thickness, and provides a good agreement between the experimental and predicted size of dendrimersome.

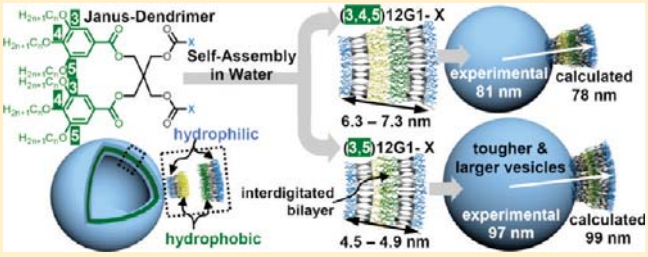

INTRODUCTION

Unilamellar vesicles self-assembled in water from natural and synthetic phospholipids (liposomes),[1] amphiphilic block copolymers (polymersomes),[2] and more recently amphiphilic Janus dendrimers (dendrimersomes)[3] can mimic primitive and contemporary biological membranes,[4] probe cell machinery,[4,5] and can be configured into biomimetic nanocapsules with technological applications ranging from nanomedicine[6] such as gene, proteins, and drug delivery[7] and theranostics,[8] to cosmetics,[9a,b] food, and agriculture.[9c] All these technological applications require stable and monodisperse vesicles of very specific dimensions, stability in various media, impermeability, and good mechanical properties.[7,10] Even liposomes assembled from natural phospholipids in the absence of cholesterol produce polydisperse, permeable, unstable, and poor mechanical properties liposomes. Therefore, all methods for the preparation of vesicles[11] require multiple fractionations most conveniently by extrusion[11g] in order to generate vesicles of specific size and polydispersity. Amphiphilic Janus dendrimers have been discovered to produce monodisperse, stable in time up to one year, and impermeable dendrimersomes with excellent mechanical properties by simple injection of their ethanol solution in water or in a buffer.[3] The ethanol injection represents the simplest method to produce vesicles from phospholipids. This procedure eliminates the oxidation and degradation of phospholipids produced by high energy sonication.[11e] However, liposomes prepared by this method require stabilization and fractionation by one of the classic methods.[11]

The mechanism of formation of vesicles is not completely elucidated, although sporadically both examples of monodisperse and stable vesicles were reported.[12] Therefore, any methodology that can predict the size of monodisperse, polydispersity, and physical properties of vesicles from the primary structure of their precursors or even by using empirical rules would endow progress in this field. This publication reports the first attempt to correlate the size and physical properties of monodisperse and stable dendrimersomes self-assembled by the ethanol injection method with the primary structure of the amphiphilic Janus dendrimer and with the morphology of their periodic arrays self-organized in bulk state. Eleven libraries containing 108 amphiphilic

Received: September 16, 2011

   dx.doi.org/10.1021/ja208762u | *J. Am. Chem. Soc.* XXXX, XXX, 000–000

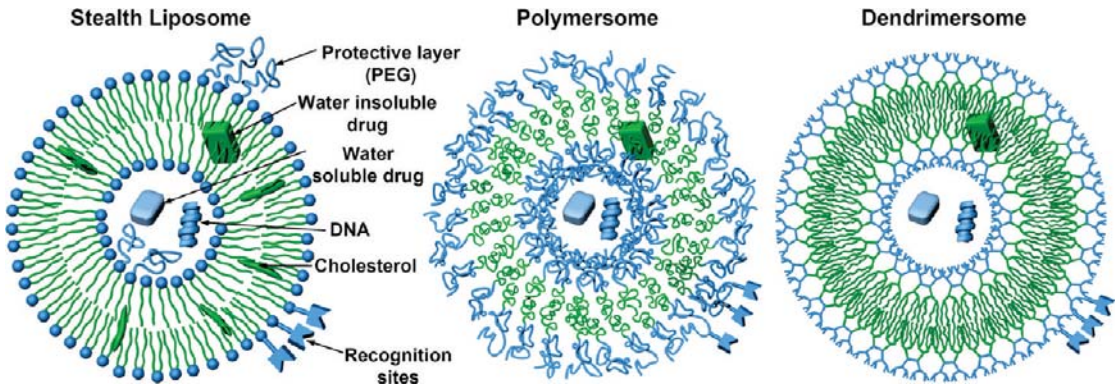

Figure 1. Summary of selected strategies to stable vesicles. Stealth liposomes co-assembled from phospholipids with phospholipids conjugated with water-soluble poly(ethylene glycole) and cholesterol (left). Polymersomes assembled from block-copolymers (middle). Dendrimersomes assembled from amphiphilic Janus dendrimers (right). The color code used is: green for the hydrophobic parts and blue for the hydrophilic parts.

Janus dendrimers were analyzed in bulk state by a combination of differential scanning calorimetry (DSC) and X-ray diffraction (XRD) experiments, and in water by dynamic light scattering (DLS) and cryo-transmission electron microscopy (cryo-TEM). A remarkable correlation of the primary structure with the structure generated in bulk and in water, both at room temperature, was discovered. On the basis of this correlation, a methodology to predict the size and some properties of the monodisperse dendrimersomes was elaborated.

RESULTS AND DISCUSSION

A Brief Discussion of the Methods To Stabilize Vesicles. As briefly mentioned in the Introduction, the stability in time, in a variety of media, and as a function of temperature of the liposomes generated from natural and synthetic phospholipids decreases in the absence of cholesterol, especially in serum.[13] Early successful attempts to stabilized liposomes involved polymerization of a 2D network in the hydrophobic part of the unilamellar structure of their membrane[13,14] and interactions of the liposome with charged synthetic polymers.[15] The most recent and most successful attempts to stabilized liposomes and vesicles are summarized in Figure 1.

Co-assembly of phospholipids with phospholipids conjugated to a water-soluble polymer such as poly (ethylene glycol) (PEG) and cholesterole leads to a class of liposomes known as sterically stabilized liposomes or Stealth liposomes.[16] Sterically stabilized liposomes (left side of Figure 1) require the co-assembly with cholesterol in their hydrophobic part in order to mediate good mechanical properties and decrease the membrane permeability. Stealth liposomes are already used commercially for the intravenous delivery of cancer drugs.[7a,e,16] Additional examples of liposomes with improved membrane properties involve phospholipids based on cholesterol as their hydrophobic part.[17] Polymersomes (middle part of Figure 1) are assembled from amphiphilic block copolymers.[2] They are very stable in time, exhibit good mechanical properties but are polydisperse. In addition, due to the limited solubility of most block copolymers in ethanol, their polymersomes cannot be prepared by the ethanol injection method. They are also polydisperse both as building blocks and as vesicles and their wall thickness is wider than that of liposomes. Dendrimersomes (right side of Figure 1) were recently reported from our laboratory.[3] They are assembled from monodisperse low generation (one or two) amphiphilic Janus dendrimers of lower molar mass than block copolymers. They self-assemble by ethanol injection producing monodisperse vesicles that are stable up to one year in water and in buffers at room temperature and above. Dendrimersomes exhibit also mechanical properties as good as those of polymersomes or of liposomes containing cholesterol. Other examples of vesicles assembled from dendrimer and dendrons based building blocks were reviewed.[18] All vesicles assembled from dendritic architectures including dendrimersomes are complementary to other drug delivery systems elaborated from dendritic building blocks.[19]

Self-Assembly of Amphiphilic Janus Dendrimers in Bulk. The synthesis of all amphiphilic Janus dendrimers discussed in this publication was reported previously.[3] The morphologies self-assembled in bulk by 108 amphiphilic Janus dendrimers were analyzed by a combination of differential scanning calorimetry (DSC) and X-ray diffraction (XRD) experiments. Details of their analysis as a function of temperature are available in the Supporting Information and are summarized in Supporting Tables ST1−ST5. DSC data revealed that 34 out of 46 amphiphilic Janus dendrimers functionalized with methoxylated oligoethylene glycol hydrophilic groups are liquid at 25 °C (74%). Their analysis by small-angle XRD confirmed that at 25 °C these 34 compounds are isotropic melts.

Figures 2−4 present the chemical structure of four libraries of Janus dendrimers and summarize the structural information of their self-assembled morphologies in water at 25 °C and in bulk at 25 °C or as close to it as accessible. It must be mentioned that the thickness of the lamellae shows a small change in this temperature range (Supporting Tables ST1−ST5). This change does not affect the trend observed and the conclusion of this report. Supporting Figure SF1 details a similar summary for the libraries 5−11. Supporting Tables ST1−ST5 summarize the detailed results of the structural characterization by XRD of 72 compounds exhibiting lamellar (47 structures), columnar hexagonal (17), columnar hexagonal superlattice[20] (1), columnar rectangular (22), cubic (1 $Pm\bar{3}n$[21] and 5 $Ia\bar{3}d$[20a,21a,22] cubic), $P4_2/mnm$ tetragonal[23] (1), and 12-fold quasi-periodic[24] (1) phases. Considering that the molecular structure of the amphiphilic Janus dendrimers investigated (Figures 2−4) can be approximated by a sheet-like shape, upon self-assembly, they are expected to generate predominantly lamellar structures.[25] The experimental results determined by XRD demonstrated that at 25 °C the lamellar phase is formed at low temperature by more than 65% of the Janus dendrimers.

dx.doi.org/10.1021/ja208762u | J. Am. Chem. Soc. XXXX, XXX, 000–000

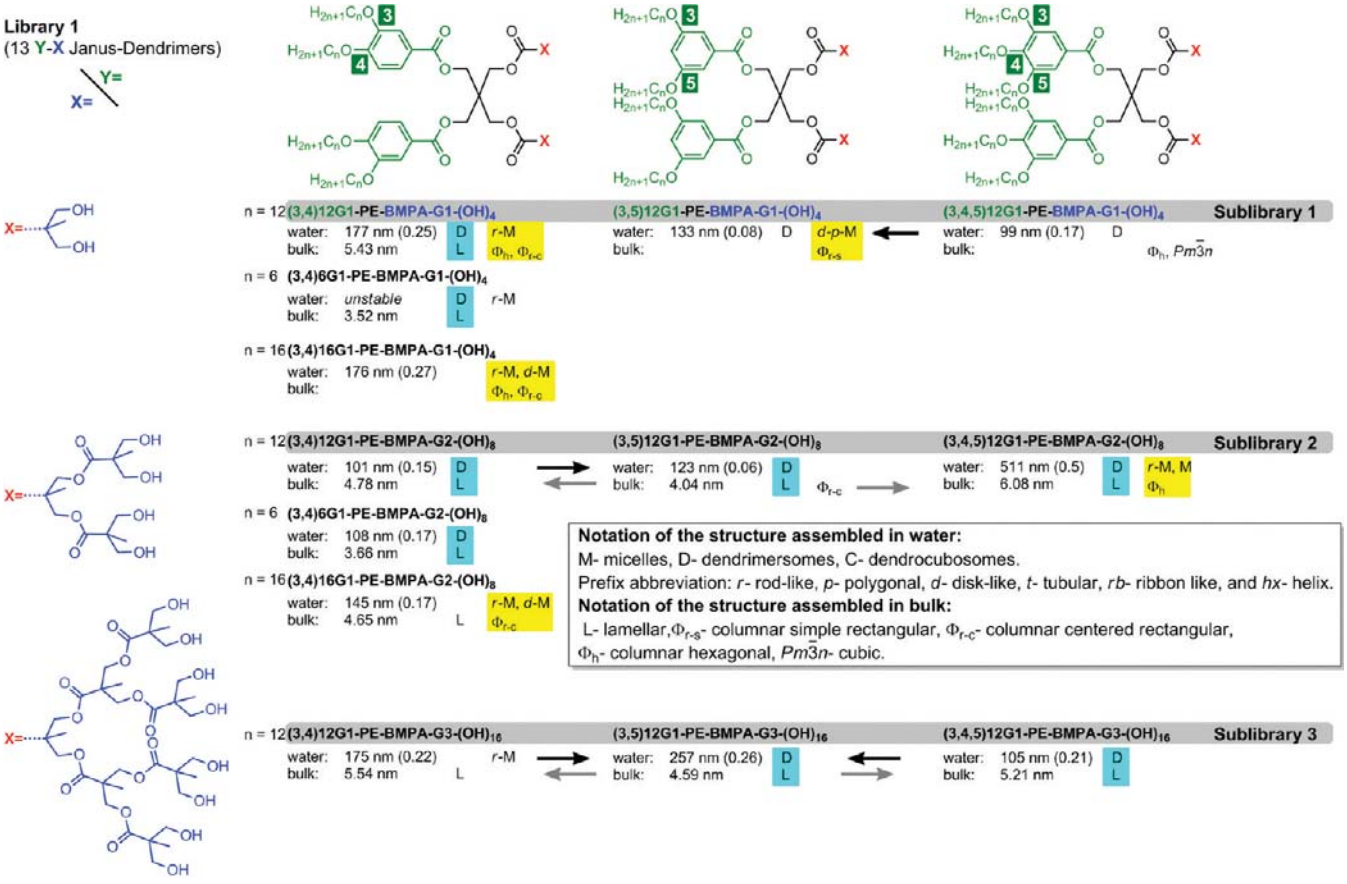

Figure 2. Structures of the amphiphilic Janus dendrimers from library 1, their short notations, and the summary of their self-assembly in water at 25 °C and in bulk state in the order of their increasing temperature. The size (in nm), polydispersity (in between parentheses), the morphologies self-assembled in water and in bulk, and the thickness of the lamellae from bulk (in nm) are indicated. When more than one structure is reported in water, it was obtained by a different method (ref 3). The black arrows illustrate the increase of the size of the structures assembled in water. The gray arrows indicate the increase of the lattice parameter of the lamellar phases formed in bulk as close as accessible to or at 25 °C. The light blue and yellow shades mark the correlations between structures in bulk and in water. Additional details are in Supporting Tables ST1−ST5.

The detailed analysis and structural characterization of the columnar, cubic, quasi-periodic, and tetragonal phases discovered in these 11 libraries of Janus-dendrimers will be reported elsewhere. In this report, our analysis is concentrated primarily on the lamellar structures self-organized from Janus-dendrimers at about 25 °C, as their structural characterization is relevant to our goal of characterizing, understanding, and predicting the formation of unilamellar dendrimersomes in water at the same temperature.

An inspection of the XRD data of the lamellar phase reported in Figures 2−4 at 25 °C or as close to it as accessible and in Supporting Tables ST1−ST5 also at other temperatures reveals an important trend between the molecular structure of the Janus dendrimers and the thickness of the lamellae at 25 °C. With no exception, the lattice parameter d_{001} of the lamellar phase formed by Janus dendrimers, which corresponds also to the layer thickness, follows the trend given by eqs 1 and 2. Because of their denser packing, the difference between the layer thickness of (3,4)nG1-X and (3,4,5)nG1-X is much less affected by the architecture of their hydrophobic branching point, although the 3,4,5-pattern shows in most cases lower thickness values than the 3,4-branching pattern. However, in very few examples, particularly, at higher generations of the hydrophilic part of the Janus dendrimer, these two hydrophobic patterns show equal or even reversed lamellae thickness. This difference is so small that it could be at the limit of the method and it is also from too small number of experimental data in order to be conclusive (compare Figures 2 and 4). Therefore, more research is required to clarify the difference between the 3,4 and 3,4,5-hydrophobic branching patterns.

$$\text{layer thickness}_{(3,4)\text{nG1}-\text{X}} > \text{layer thickness}_{(3,5)\text{nG1}-\text{X}} \quad (1)$$

$$\text{layer thickness}_{(3,4,5)\text{nG1}-\text{X}} > \text{layer thickness}_{(3,5)\text{nG1}-\text{X}} \quad (2)$$

In eqs 1 and 2, X denotes the structure of the hydrophilic part of the Janus dendrimer, as illustrated in the left side of Figures 2−4. For a specific hydrophilic structure of the Janus dendrimer, these correlations demonstrate that the lattice parameter of the lamellar phase is controlled by the branching pattern of the hydrophobic part. Furthermore, this dependence demonstrates that the (3,5)nG1- branching pattern of the alkyl chains generates layers with smaller thickness than the (3,4)nG1- and (3,4,5)nG1-. This suggests a more interdigitated packing of the layers forming the lamellar phase self-organized from (3,5)nG1-X Janus dendrimers. Therefore, the structural characterization of 108 Janus dendrimers was organized in Figures 2−4 in order to follow the structure of their hydrophobic and hydrophilic part. In addition

dx.doi.org/10.1021/ja208762u | J. Am. Chem. Soc. XXXX, XXX, 000–000

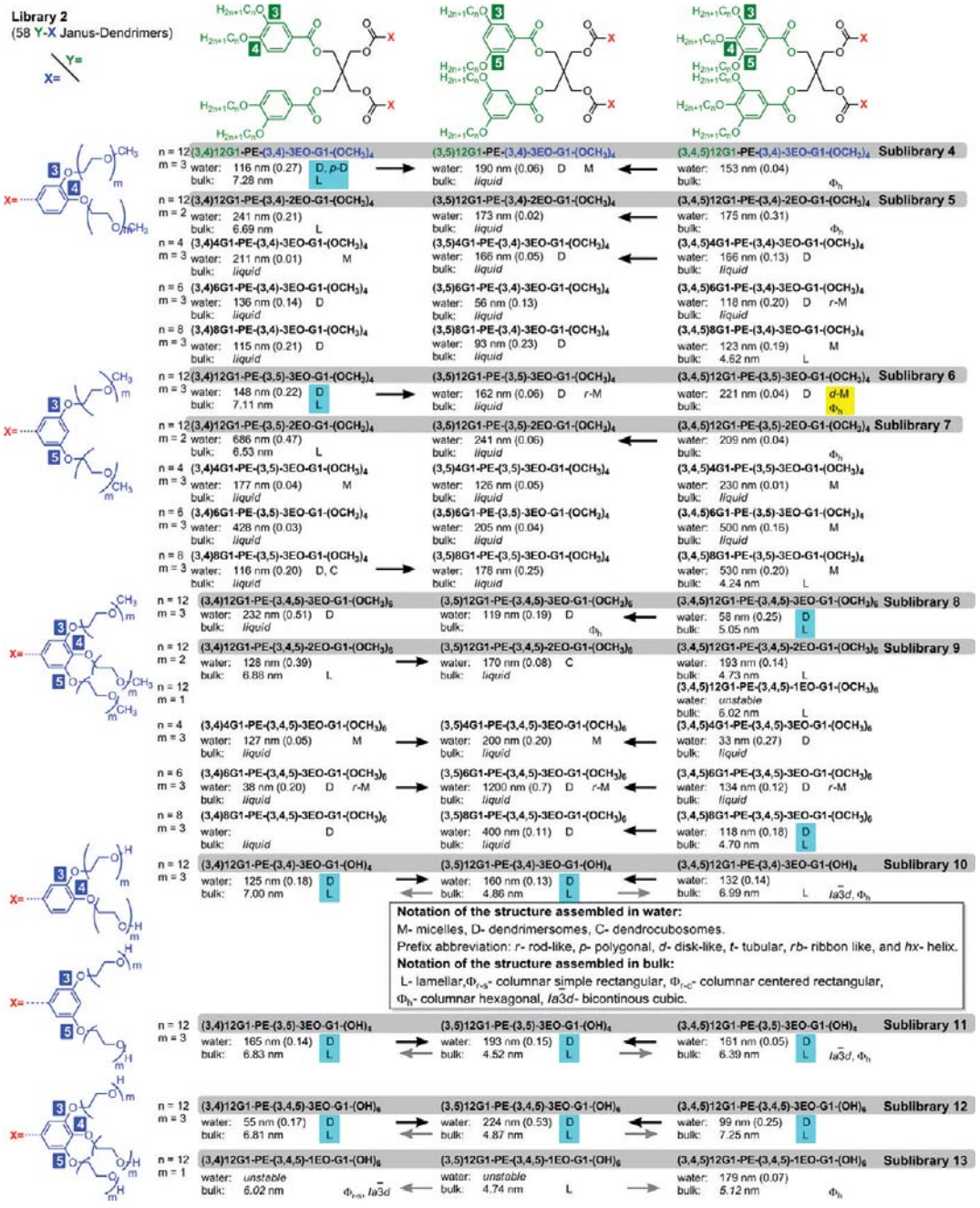

Figure 3. Structures of the amphiphilic Janus dendrimers from library 2, their short notations, and the summary of their self-assembly in water at 25 °C and in bulk state in the order of their increasing temperature. The size (in nm), polydispersity (in between parentheses), the morphologies self-assembled in water and in bulk, and the thickness of the lamellae from bulk (in nm) are indicated. When more than one structure is reported in water, it was obtained by a different method (ref 3). The black arrows illustrate the increase of the size of the structures assembled in water. The gray arrows indicate the increase of the lattice parameter of the lamellar phases formed in bulk as close as accessible to or at 25 °C. The light blue and yellow shades mark the correlations between structures in bulk and in water. Additional details are in Supporting Tables ST1−ST5.

to the molecular structures, Figures 2−4 detail the structural parameters determined in water at 25 °C, listed in the order: size by DLS, polydispersity, and type of morphology defined in Supporting Tables ST1− ST5 and also in Figures 2−4, as well as the structural parameters determined by XRD in solid state at 25 °C, listed in the order: d_{001} and phases in the order of increasing temperature as defined in Supporting Tables ST1−ST5.

The gray arrows shown in Figures 2−4 indicate the increase of the lattice parameter d_{001} of the lamellar phase, observed for all the sublibraries of Janus dendrimers. In this report, a sublibrary of Janus dendrimers is defined by the three structures that correspond to three branching patterns for the hydrophobic part, (3,4)-, (3,5)-, and (3,4,5)-, respectively, while the structure of the hydrophilic part is identical. For example, the top of Figures 2−4 show the structure and branching pattern of the hydrophobic part of the amphiphile (green color). In the left side of Figures 2−4, for each sublibrary of Janus dendrimers, the structure of their hydrophilic part is detailed (blue color).

dx.doi.org/10.1021/ja208762u | J. Am. Chem. Soc. XXXX, XXX, 000–000

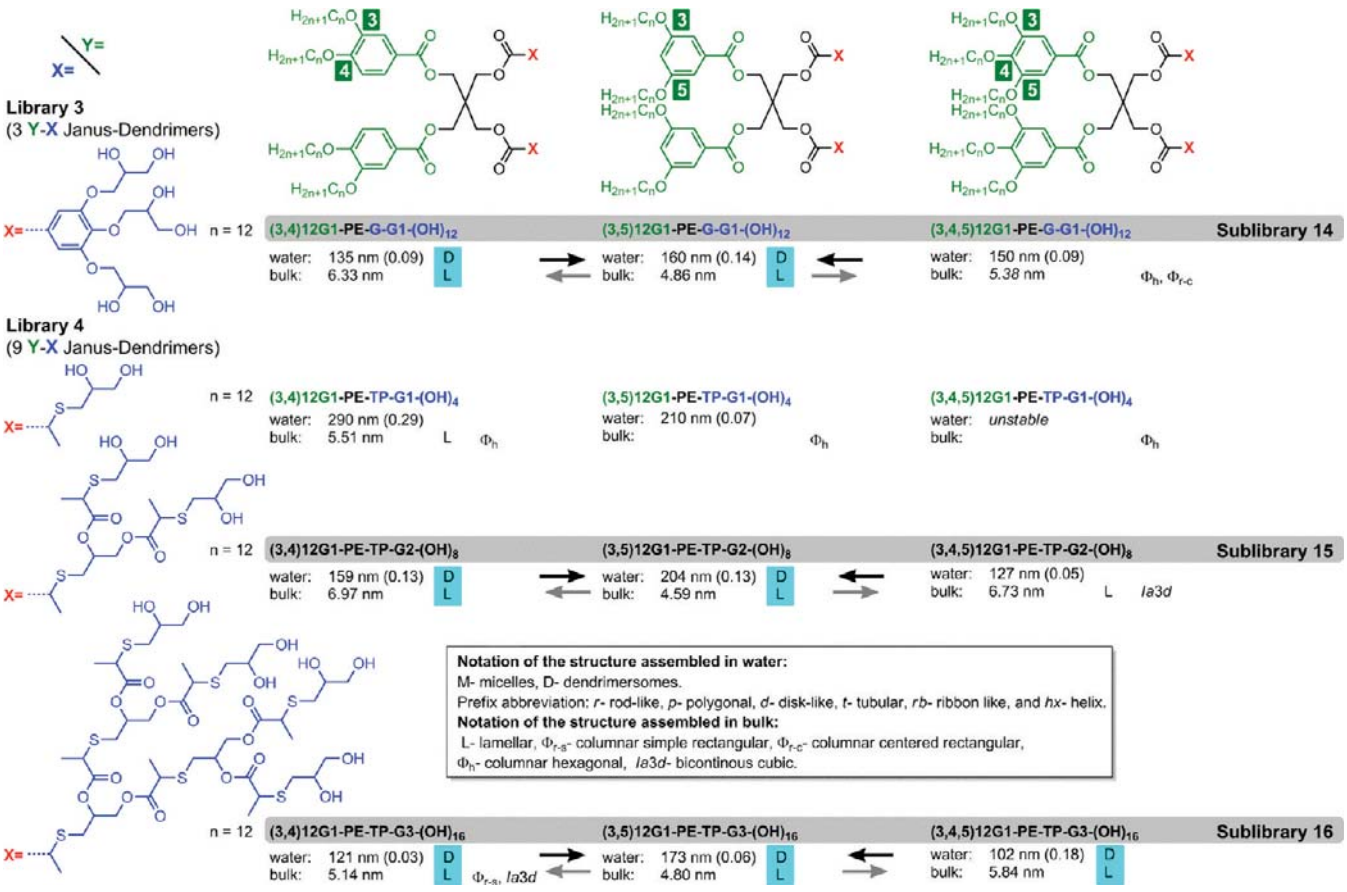

Figure 4. Structures of the amphiphilic Janus dendrimers from libraries 3 and 4, their short notations, and the summary of their self-assembly in water at 25 °C and in bulk state in the order of their increasing temperature. The size (in nm), polydispersity (in between parentheses), the morphologies self-assembled in water and in bulk, and the thickness of the lamellae from bulk (in nm) are indicated. The black arrows illustrate the increase of the size of the structures assembled in water. The gray arrows indicate the increase of the lattice parameter of the lamellar phases formed in bulk as close as accessible to or at 25 °C. The light blue and yellow shades mark the correlations between structures in bulk and in water. Additional details are in Supporting Tables ST1−ST5.

Figure 5 shows typical powder XRD data observed for a sublibrary of Janus dendrimers forming lamellar phases. The lattice parameter d_{001} of (3,4)12G1-PE-TP-G2-$(OH)_8$ and (3,4,5)12G1-PE-TP-G2-$(OH)_8$ Janus-dendrimers are relatively close, 69.7 and 67.3 Å, respectively (Figure 5a). However, these two values are, by 34% and 32%, respectively, larger than the 45.9 Å lattice parameter of the lamellar phase formed by (3,5)12G1-PE-TP-G2-$(OH)_8$ Janus dendrimer. The reconstructed relative electron density distributions shown in Figure 5b illustrate the significant reduction of the thickness of the low electron density region, marked in green, which corresponds to the aliphatic part of the Janus dendrimer (3,5)12G1-PE-TP-G2-$(OH)_8$. The molecular models of the sublibrary 15 of Janus dendrimers **Y**-PE-TP-G2-$(OH)_8$, shown in Figure 5c, demonstrates the more interdigitated packing of the aliphatic chains[26] in the lamellar structure of **(3,5)12G1**-PE-TP-G2-$(OH)_8$ in comparison with **(3,4,5)12G1**-PE-TP-G2-$(OH)_8$ and **(3,4)12G1**-PE-TP-G2-$(OH)_8$. The 3,4,5-branching pattern gives only slightly better packing than the 3,4-based architecture. The clarification of this small difference requires additional research.

A similar trend that correlates the lattice parameter of the lamellar phases and the branching pattern of the hydrophilic part of the Janus-dendrimers can be established from the XRD data summarized in Supporting Tables ST1−ST5 and Figures 2−4. Nevertheless, the systematic change of thickness between the three branching patterns of the hydrophilic part, -(3,4)nEO-, -(3,5)nEO, and -(3,4,5)nEO-, respectively, seems to be less significant (Figure 6). This effect is diminished most probably due to the increased conformational freedom of the oligoethylene glycol chains in comparison with the alkyl chains, within the same temperature range. The difference between the length of the hydrophobic and hydrophilic chains can also account for the diminishing effect of the branching pattern of the oligoethylene glycol chains to the thickness of bilayer but to a lesser extent. This is supported by the observation that the thickness of the layers can be increased by a roughly 3 or 4 times larger percentage via changes of the branching pattern of the alkyl chains. For example, in Figure 6a, the thickness of the layers were increased only by 7.5−13.5% due to the change of the branching pattern of the hydrophilic chains versus 41.4−48.8% due to the branching pattern of the hydrophobic chains. On the other hand, the difference in the length of a C12 alkyl chain and of a 3EO hydrophilic chain in an all-*trans* conformation of approximately 25% cannot provide by itself such significant differences. For example, the thickness of the layers formed by (3,4,5)12G1-PE-(**3,4**)-3EO-G1-$(OH)_4$, 6.99 nm, and (3,4,5)12G1-PE-(**3,4,5**)-3EO-G1-$(OH)_4$, 7.25 nm, is larger than the 6.39 nm layer thickness for (3,4,5)12G1-PE-(**3,5**)-3EO-G1-$(OH)_4$, but just by only 9.4%

dx.doi.org/10.1021/ja208762u | *J. Am. Chem. Soc.* XXXX, XXX, 000–000

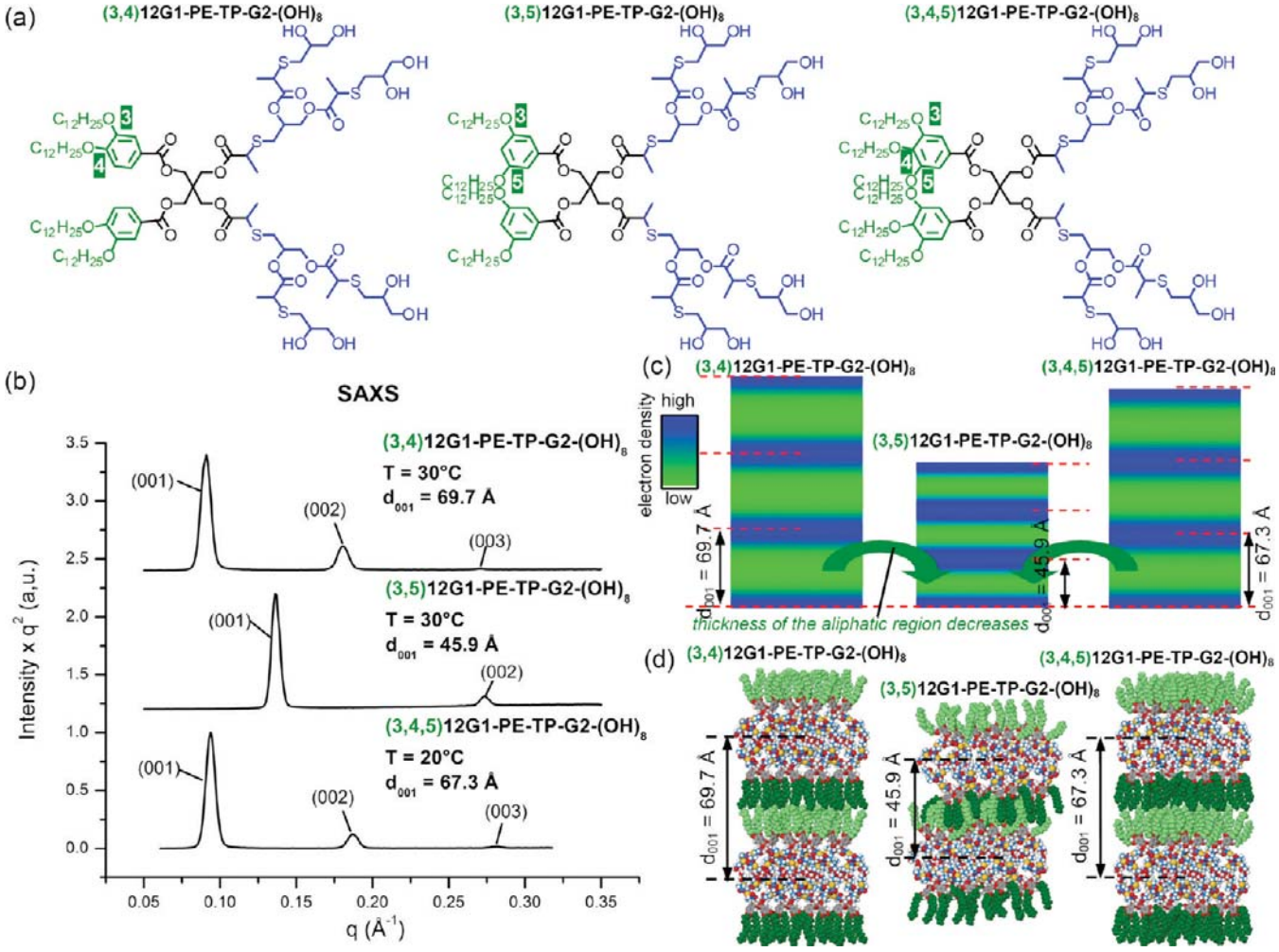

Figure 5. Structures (a) and the corresponding powder XRD data collected in the lamellar phases of the indicated amphiphilic Janus dendrimers (b). Reconstructed relative electron density maps (c) illustrating the change of the thickness of the layer from the less interdigitated (3,4)12G1-X and (3,4,5)12G1-X to the more interdigitated (3,5)12G1-X amphiphilic Janus dendrimers (d).

and 13.5%, respectively. Figure 6 summarizes this general trend that the thickness of the layers forming lamellar phases is templated by the branching pattern of both hydrophobic and hydrophilic part of the Janus-dendrimers.

Correlations between the Supramolecular Structures Formed by Self-Assembling Amphiphilic Janus-Dendrimers in Bulk and in Water. The combined analysis of the structures assembled in water and in solid state, summarized in Figures 2−4 and Supporting Tables ST1−ST5, revealed some similarities between the two self-assembly processes. The large majority of Janus-dendrimers forming lamellar phases in bulk also formed vesicles in water (83.3%, Table 1). Only 13.8% of the structures forming lamellar phases in bulk formed nonvesicular morphologies in water. On the other hand, more than half of the Janus-dendrimers exhibiting columnar or cubic phases in bulk also formed micellar structures in water (52.2%, Table 1). These results demonstrate that at the same temperature there is a direct correlation between the structures formed by Janus-dendrimers in bulk and in water. This correlation is affected by the hydration and swelling of the hydrophilic part of the Janus dendrimer and by the hydrophobic effect that are expected to compress the thickness of the hydrophobic part of the membrane in the dendrimersome. However, in spite of this effect, the experimental correlation is remarkable.

The formation of lamellar phases in bulk implies that these amphiphilic Janus dendrimers are favoring the formation of bilayer structures with small surface curvature.[25] This implies that in the case of self-assembly in water, these Janus-dendrimers should favor the formation of vesicles and disfavor the formation of micelles. The self-assembly into micelles in water is disfavored because their formation require a large penalty to their free energy minimum generated by the large surface curvature of the assembly.[2f,27] On the other hand, Janus-dendrimers forming columnar or cubic phases in bulk are expected to predominantly form micellar structures in water, as in both columnar and cubic phases, the primary structure of the amphiphilic Janus dendrimer favors the formation of structures with large surface curvature.

The self-assembly process in water is dominated by the hydrophilic−hydrophobic interactions acting between the Janus-dendrimer and the polar medium. These interactions are absent in the case of the self-assembly of Janus-dendrimers in bulk. Therefore, this additional layer of interactions to the self-assembly process can favor the formation of dendrimersomes in water for a larger fraction of structures exhibiting columnar or

dx.doi.org/10.1021/ja208762u |J. Am. Chem. Soc. XXXX, XXX, 000–000

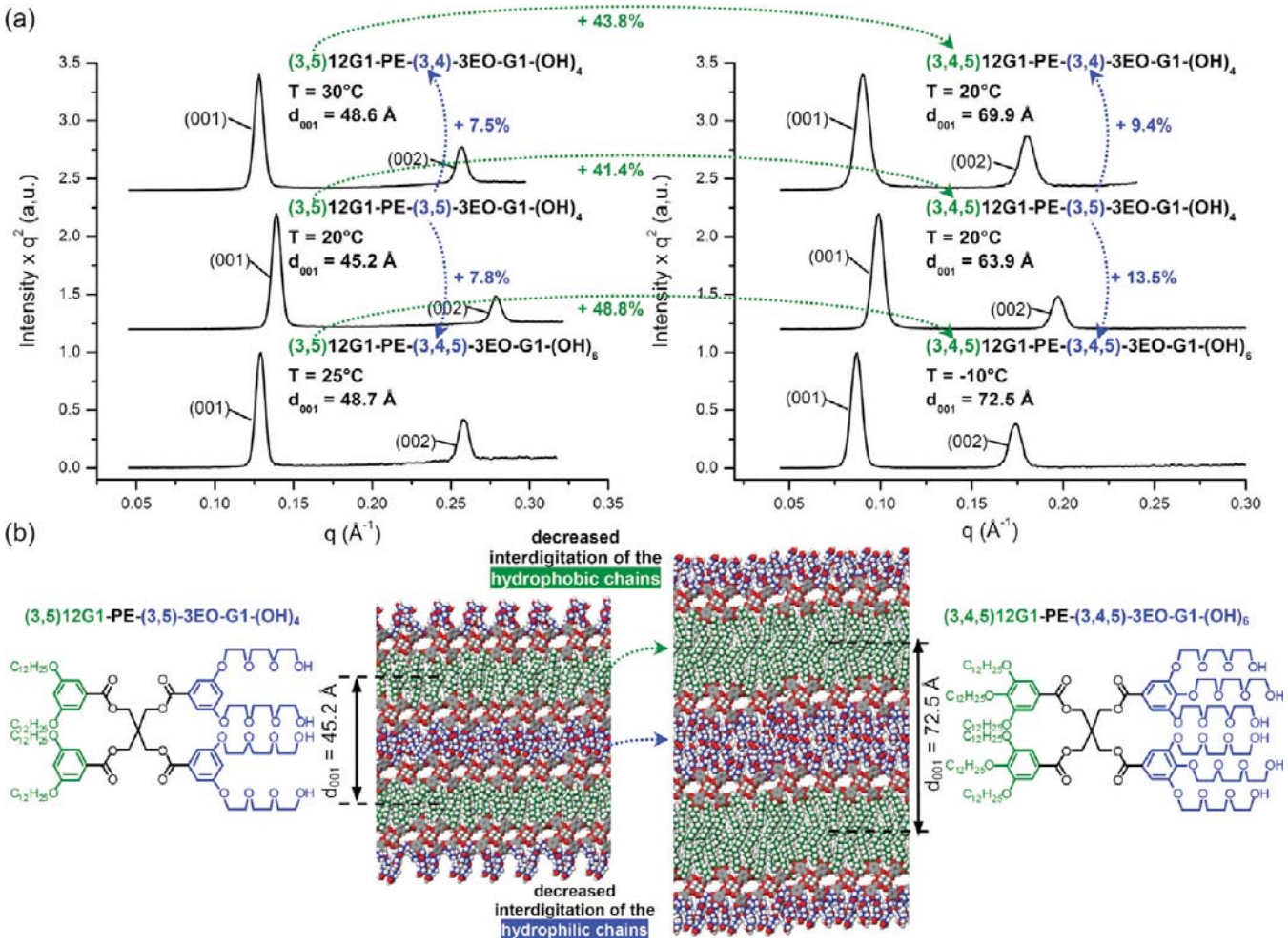

Figure 6. Powder XRD data collected in the lamellar phases of the indicated amphiphilic Janus dendrimers (a) and corresponding molecular models shown at scale (b). In (a), the dotted arrows indicate the systematic increase of the thickness of the supramolecular layers which follow the branching pattern of the hydrophobic (green) and hydrophilic (blue) part of the amphiphilic Janus dendrimers.

Table 1. Correlation between the Structure Self-Assembled in Bulk and in Water Established from the Analysis of 50 Amphiphilic Janus Dendrimers[a]

structure assembled in bulk [number of dendrimers]	structure assembled in water [number of dendrimers]	correlation between structure assembled in bulk and in water	percentage from the total number of structures assembled in water[b]
lamellar [36]	dendrimersomes [30]	30/36 = 83.3%	53.6%
columnar/cubic [23]	dendrimersomes [9]	9/23 = 39.1%	16.0%
lamellar [36]	micelles [5]	5/36 = 13.8%	8.9%
columnar/cubic [23]	micelles [12]	12/23 = 52.2%	21.4%

[a] Data calculated from 50 structures analyzed by all methods (XRD and CRE, GUD, CryoTEM). [b] Percentage calculated from the number of dendrimers forming the structure in water divided by 30 + 9 + 5 + 12 = 56; from the total of 50 Janus dendrimers, 8 exhibit both dendrimersome and micellar-like structures in water.

cubic phases in solid state (39.1%, Table 1). This process is generated by the interaction with the water medium that provides the additional energy needed to compensate for the formation of surfaces with smaller curvature, which are disfavored in solid state. For example, the interaction with the polar medium reduces the mean curvature[25] (c_m) from ~0.2 nm^{-1} (in bulk $c_m = 1/D_{column} \sim 1/(5.0\ nm) = 0.2\ nm^{-1}$; the column diameter D_{column} listed in Supporting Tables ST1−ST5) to ~0.02 nm^{-1} (in water $c_m = 2/D_{vesicle} \sim 1/(50.0\ nm) = 0.02\ nm^{-1}$; the vesicle diameter listed in Figures 2−4). Similarly, a very small percentage of Janus-dendrimers exhibiting lamellar phases in bulk are forming micellar structures in water (13.8%, Table 1), because only in few cases the interaction with water is sufficiently strong to compensate for the change from surfaces with small curvature, which are favored in solid state, to surfaces with large curvature characteristic for the rod, tubular, and micellar structures formed in water. For example, in this case, the interaction with the polar medium must compensate for a larger change of the mean curvature from $c_m^{(lamellar)} = 0\ nm^{-1}$ to ~0.2 nm^{-1}.

dx.doi.org/10.1021/ja208762u | J. Am. Chem. Soc. XXXX, XXX, 000–000

Table 2. Correlation between the Substitution Pattern of the Hydrophobic Part, Y= (3,4)12G1-, (3,5)12G1-, and (3,4,5)12G1-, Containing Dodecyl Alkyl Groups from 16 Constant Generation Number of the Hydrophilic Part (X) of the Amphiphilic Janus Dendrimer and the Radius of the Dendrimersomes Self-Assembled in Water[a]

correlation of the radius of the dendrimersome with their (3,4)12G1-, (3,5)12G1-, and (3,4,5)12G1- substitution pattern	number of sublibraries following the correlation	percentage
R_{DLS}\{(3,4)12G1-X\} < R_{DLS}\{(3,5)12G1-X\}	12	12/16 = 75%
R_{DLS}\{(3,5)12G1-X\} > R_{DLS}\{(3,4,5)12G1-X\}	12	12/16 = 75%
R_{DLS}\{(3,4)12G1-X\} < R_{DLS}\{(3,5)12G1-X\} and R_{DLS}\{(3,5)12G1-X\} > R_{DLS}\{(3,4,5)12G1-X\}	8	8/16 = 50%

[a] Data calculated from the DLS analysis of the 16 sublibraries reported in Figures 2−4.

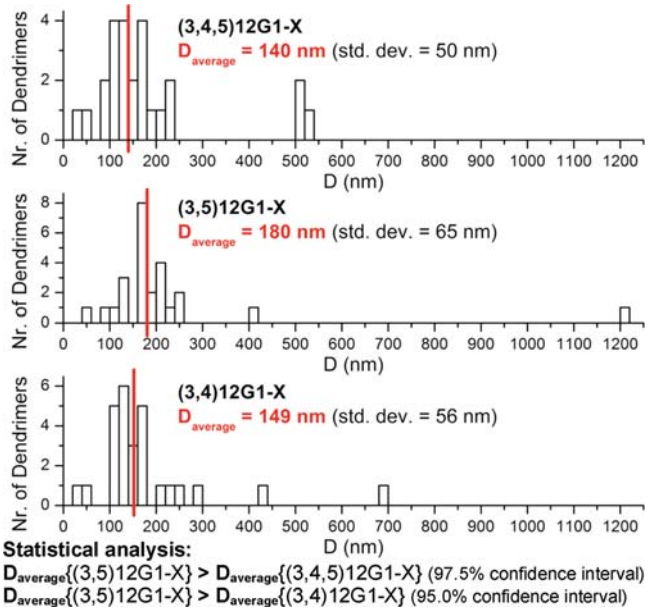

Figure 7. Histograms of the size of dendrimersomes determined by DLS for the libraries 1−4 from Figures 2−4, separated as a function of the structure of the hydrophobic part of the amphiphilic Janus dendrimer. In all cases, the average size and standard deviation are indicated.

Knowing that in solid state we established a direct proportionality between the branching pattern of the hydrophobic or hydrophilic part of the Janus-dendrimer and the thickness of the layers self-organized into lamellar structures, we now focus on establishing if this trend is preserved by their self-assembly in water and, if it is preserved, what are its consequences. The thickness of the vesicle wall, determined previously by cryo-TEM,[3] confirmed that the eqs 1 and 2 are also valid for the dendrimersome structures self-assembled in water.

The size of the dendrimersomes calculated from the DLS data reported in Figures 2−4 follows a trend that demonstrates an inverse proportionality between the thickness of the vesicle wall and the diameter of the vesicle. These correlations are indicated in Figures 2−4 by the gray arrows that follow the increase of the bilayer thickness (d_{001} listed in the figures and also in Supporting Tables ST1−ST5), and by the black arrows that follow the increase of the diameter of the vesicles. In 75% of the 16 sublibraries of Janus-dendrimers summarized in Table 2, the size of the dendrimersomes formed by structures with (3,4)12G1- and (3,4,5)12G1- branching pattern for the hydrophobic part is smaller than the size of those based on the (3,5)12G1- hydrophobic substitution pattern. The fact that the trends established for the self-assembly of Janus dendrimers in bulk, eqs 1 and 2, are preserved by their self-assembly in water is somewhat expected considering that their additional interaction with the polar medium should not have a significant effect to the packing of the hydrophobic region. Once the dendrimersome structure forms, the inner hydrophobic region of the vesicle wall is shielded from the interaction with the water medium by the hydrophilic groups of Janus dendrimers.

The combined statistical analysis of the size of the dendrimersomes reported in Figure 7 for all the amphiphilic Janus dendrimers from the libraries 1−4, illustrates that the average size of the vesicles formed from the (3,5)12G1-X type of Janus structures is larger than those formed by the (3,4,5)12G1-X and (3,4)12G1-X type of structures. These differences were shown to be statistically significant. The statistical confidence interval is indicated in Figure 7. Furthermore, the mechanical properties reported previously for dendrimersomes demonstrated that the their elastic area expansion modulus, lysis tension, and energy stored at failure increase significantly upon the change from (3,4,5)12G1-X to (3,4)12G1-X, in some cases by a factor of 20, and also increase upon the change from (3,4)12G1-X to (3,5)12G1-X, in some cases by a factor of 2.[3] Moreover, although the dendrimersomes formed in water are very stable (their structures was shown to be unchanged for more than 12 months), consistently the only dendrimersomes exhibiting a significant time variation of their size were those formed by (3,4,5)12G1-X.[3]

The results presented in Figures 2−7 demonstrate that the molecular structure of amphiphilic Janus dendrimers, specifically the branching pattern of their hydrophobic part, templates the size, stability, and mechanical properties of the dendrimersome structure formed in water. Therefore, the increased stability, membrane tension, elastic area expansion modulus, and energy stored at failure of the vesicles formed by (3,5)12G1-X and (3,4)12G1-X Janus-dendrimers[3] are determined by their increased degree of interdigitation within the hydrophobic part of the membrane in comparison with the (3,4,5)12G1-X structures (Figures 5 and 6). This trend is expected considering that a more interdigitated structure of the vesicle wall is most probably more stable and significantly harder to bend or to fracture than a less interdigitated structure.

The elastic bending module and lysis tension of liposomes was shown previously to increase proportionally with the decrease of unsaturation of the alkyl chains.[28a,29] For polymersomes, the membrane lysis tension was shown to increase with the molecular weight and thickness.[30] These results show a variety of structural parameters that can be tuned to improve membrane stability. In the case of dendrimersomes, a remarkable stability and membrane strength was achieved by varying the substitution pattern of the hydrophobic part of the amphiphile, while keeping the membrane thickness in a narrow range of ~3−5 nm.[3] These

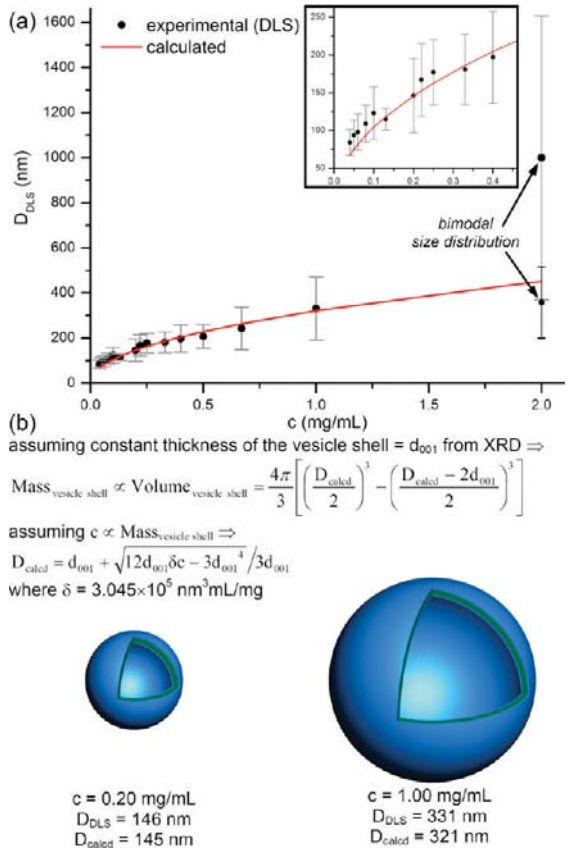

Figure 8. The dependence of the diameter determined by DLS, D_{DLS}, of the monodisperse dendrimersomes and the concentration, c, of the (3,5)12G1-PE-BMPA-G2-$(OH)_8$ amphiphilic Janus dendrimer in water (a). Schematic of the simplified vesicle model used to fit the experimental data (b). The inset from (a) shows an enlargement of the dependence at low concentrations. Dendrimersomes were prepared by the injection of amphiphilic Janus dendrimer from ethanol solution in water.

two structural features are of great interest for biomimetic membrane applications.[31,32]

The fact that statistically (Figure 7) the largest vesicles are those formed by the (3,5)12G1-X branching pattern of the amphiphilic Janus dendrimers can be attributed to the increased mechanical strength of a more interdigitated bilayer structure, that favors the formation of surfaces with smaller curvature (e.g., larger dendrimersomes). As it will be shown in the next subsection, the dependence established between the primary structure of the amphiphilic Janus dendrimer and their structure formed either in solid state or in water medium will be used to predict the size of the vesicle.

Predicting the Size of the Monodisperse Dendrimersomes Formed in Water by Self-Assembling Amphiphilic Janus Dendrimers. The diameter of the dendrimersomes (D_{DLS}) formed by the injection of the ethanol solution of (3,5)12G1-PE-BMPA-G2-$(OH)_8$ increases with their concentration, c (Figure 8a). Since D_{DLS} is calculated from the hydrodynamic radius, the actual diameter of the dendrimersome will be slightly overestimated. However, this effect is expected to be small and have no effect on the overall trend discussed here. The formation of dendrimersomes by the injection method is a fast self-assembling process. On the other hand, the (3,5)12G1-PE-BMPA-G2-$(OH)_8$ Janus-dendrimer was shown to form giant unilamellar dendrimersomes via the film hydration method.[3] Therefore, depending on the preparation method, the size of the dendrimersomes formed by (3,5)12G1-PE-BMPA-G2-$(OH)_8$ Janus-dendrimer can be varied through a remarkable range of 2 orders of magnitude, from ~100−300 nm (Figure 8) to 20 μm.[3] This large range of sizes suggests that under the preparation conditions reported in Figure 8, the dendrimersomes self-assembled from (3,5)12G1-PE-BMPA-G2-$(OH)_8$ Janus dendrimers did not yet reach the curvature limit and that their size dependence is determined by the local concentration. This curvature limit[2f,12g,27] is an intrinsic property of the system, (Janus dendrimer) + (concentration) + (polar medium), that depending on these three parameters might restrict any subsequent decrease or increase of the size of the dendrimersomes. Clearly, in the range of concentrations reported in Figure 8, the self-assembly process has not yet reach the regime corresponding to either the smallest or largest dendrimersome. This size-concentration dependence of the self-assembled dendrimersomes follows similar proportionalities observed in other natural and synthetic-based vesicles.[33]

Assuming that the dendrimersomes are perfect spheres (Figure 8b) with uniform thickness of their shell equal to that of their lamellae from bulk state that is d_{001} (Figures 2−4 and Supporting Tables ST1−ST5), the mass of the vesicle shell can be calculated by using eq 3. The small difference between the real membrane thickness produced by hydration, solvation, and the hydrophobic effect and that of the lamellae in bulk state does not affect this trend.

$$\text{Mass}_{\text{vesicle shell}} \propto \text{Volume}_{\text{vesicle shell}} = \frac{4\pi}{3}\left[\left(\frac{D_{\text{calcd}}}{2}\right)^3 - \left(\frac{D_{\text{calcd}} - 2d_{001}}{2}\right)^3\right] \quad (3)$$

In eq 3, D_{calcd} is the calculated diameter of the vesicle. Assuming a direct proportionality between the concentration of Janus-dendrimers, c, and the mass of the vesicle shell (eq 4), the diameter of the dendrimersome is given by eq 5. Equation 5 was deduced by solving the system of eqs 3 and 4.

$$c \propto \text{Mass}_{\text{vesicle shell}} \quad (4)$$

$$D_{\text{calcd}} = d_{001} + \sqrt{12d_{001}\delta c - 3d_{001}^4}/(3d_{001}) \quad (5)$$

In eq 5, the fitting parameter δ is the concentration proportionality factor. Figure 8a details the agreement between the experimental diameter of the dendrimersomes determined by DLS and the calculated diameter based on eq 5 with $\delta = 3.045 \times 10^5$ nm^3 mL/mg. This result confirms that the assumption from eq 4 is valid. Under the conditions that the dendrimersomes self-assembled in water from various amphiphilic Janus dendrimers prepared using the same concentration, eq 4 provides eq 6.

$$\text{Mass}_{\text{vesicle shell}}{}^{\text{ref str}} = \text{Mass}_{\text{vesicle shell}}{}^{\text{calcd}} \quad (6)$$

Equation 6 is used to predict the size of the dendrimersome, R_{calcd}, based on the size of a reference structure determined experimentally, $R_{\text{DLS}}{}^{\text{ref str}}$. From eqs 3 and 6, the predicted size of the dendrimersome is given by eq 7, with Δ given by eq 8.

$$R_{\text{calcd}} = d_{001}/2 + \sqrt{12d_{001}\Delta - 3d_{001}^4}/(6d_{001}) \quad (7)$$

$$D = [(R_{\text{DLS}}{}^{\text{ref str}})^3 - (R_{\text{DLS}}{}^{\text{ref str}} - d_{001}{}^{\text{ref str}})^3](M_{\text{wt}}{}^{\text{ref str}}/M_{\text{wt}}) \quad (8)$$

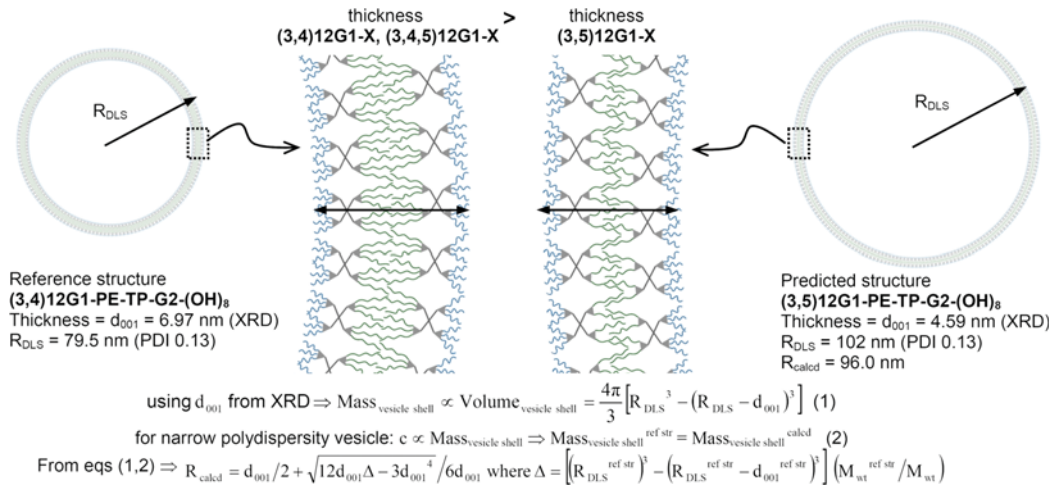

Figure 9. Calculation of the size of dendrimersomes using the combined XRD and DLS experimental data.

Table 3. Calculation of the Predicted Radius of the Dendrimersome

Janus-dendrimer	d_{001} (nm)[a]	$M_{wt}/M_{wt}^{ref\ str}$ [b]	R_{DLS} (nm)[c]	R_{calcd} [d] (nm)	correlation[e]
(3,4)12G1-PE-TP-G2-$(OH)_8$ *reference structure*	**6.97**	**1**	**79.5**	-	-
(3,5)12G1-PE-TP-G2-$(OH)_8$	4.59	1	102	96.0	yes
(3,4,5)12G1-PE-TP-G2-$(OH)_8$	6.73	1.18	63.5	74.6	yes
(3,4)12G1-PE-TP-G3-$(OH)_{16}$ *reference structure*	**5.65**	**1**	**60.5**	-	-
(3,5)12G1-PE-TP-G3-$(OH)_{16}$	5.02	1	86.5	63.7	yes
(3,4,5)12G1-PE-TP-G3-$(OH)_{16}$	5.84	1.11	51.0	56.8	yes
(3,4)12G1-PE-TP-G3-$(OH)_{16}$ *reference structure*	**5.65**	**1**	**83.0**[f]	-	-
(3,5)12G1-PE-TP-G3-$(OH)_{16}$	5.02	1	97.0[f]	90	yes
(3,4,5)12G1-PE-TP-G3-$(OH)_{16}$	5.84	1.11	67.0[f]	77.0	yes
(3,4)12G1-PE-BMPA-G2-$(OH)_8$ *reference structure*	**4.78**	**1**	**50.5**	-	-
(3,5)12G1-PE-BMPA-G2-$(OH)_8$	4.04	1	61.5	54.4	yes
(3,4)12G1-PE-BMPA-G2-$(OH)_8$ *reference structure*	**4.78**	**1**	**80.0**[f]	-	-
(3,5)12G1-PE-BMPA-G2-$(OH)_8$	4.04	1	95.0[f]	86.5	yes
(3,4)12G1-PE-BMPA-G3-$(OH)_{16}$ *reference structure*	**5.54**	**1**	**87.5**	-	-
(3,5)12G1-PE-BMPA-G3-$(OH)_{16}$	4.5	1	128.5	96.3	yes
(3,4,5)12G1-PE-BMPA-G3-$(OH)_{16}$	5.21	1.13	52.5	84.6	yes
(3,4)12G1-PE-(3,4)-3EO-G1-$(OH)_4$ *reference structure*	**7.00**	**1**	**62.5**[f]	-	-
(3,5)12G1-PE-(3,4)-3EO-G1-$(OH)_4$	4.86	1	80[f]	73.3	yes
(3,4)12G1-PE-(3,5)-3EO-G1-$(OH)_4$ *reference structure*	**6.83**	**1**	**82.5**[f]	-	
(3,5)12G1-PE-(3,5)-3EO-G1-$(OH)_4$	4.52	1	96.5[f]	99.5	yes
(3,4,5)12G1-PE-(3,5)-3EO-G1-$(OH)_4$	6.39	1.19	80.5[f]	78.0	yes
(3,4)12G1-PE-(3,4,5)-3EO-G1-$(OH)_6$ *reference structure*	**6.81**	**1**	**27.5**	-	-
(3,5)12G1-PE-(3,4,5)-3EO-G1-$(OH)_6$	4.58	1	112	31.7	yes
(3,4,5)12G1-PE-(3,4,5)-3EO-G1-$(OH)_6$	5.4	1.18	49.5	27.7	yes
(3,4)12G1-PE-G-G1-$(OH)_{12}$ *reference structure*	**6.33**	**1**	**67.5**[f]	-	-
(3,5)12G1-PE-G-G1-$(OH)_{12}$	4.86	1	80.0[f]	76.0	yes

[a] d-spacing of the lamellar phase reported in Figures 2−4 and Supporting Tables ST1−ST5. [b] Molecular weight ratio used in the prediction of the radius of the dendrimersome; the $M_{wt}^{ref\ str}$ is the molecular weight of the indicated reference structure. [c] Experimental radius of the dendrimersome; data reported in ref 3 for the experiments based on injection from ethanol. [d] Radius of the dendrimersome calculated from the combined analysis of the self-assembly process in solid state and in water: $R_{calcd} = d_{001}/2 + [12d_{001}\Delta - 3(d_{001})^4]^{1/2}/6d_{001}$ (eq 7), where $\Delta = [(R_{DLS}^{ref\ str})^3 - (R_{DLS}^{ref\ str} - d_{001}^{ref\ str})^3]\ M_{wt}^{ref\ str}/M_{wt}$ (eq 8). [e] Correlation between calculated radius of the dendrimersome and experimental radius defined as "yes" if R_{calcd} and R_{DLS} are either both larger, or both smaller than $R_{DLS}^{ref\ str}$, and defined as "no" otherwise. [f] DLS data collected by injection from tetrahydrofuran ($c = 0.25$ mg/mL = concentration of Janus-dendrimer in water).

In eqs 7 and 8: $d_{001}^{ref\ str}$ and $M_{wt}^{ref\ str}$ are, respectively, the thickness of the vesicle wall (Figures 2−4), and the molecular weight of the Janus dendrimer chosen as reference structure, while d_{001} and M_{wt} are, respectively, the thickness of the vesicle wall (Figures 2−4) and the molecular weight of the Janus-dendrimer for which the size of the dendrimersome is predicted.

dx.doi.org/10.1021/ja208762u |*J. Am. Chem. Soc.* XXXX, XXX, 000–000

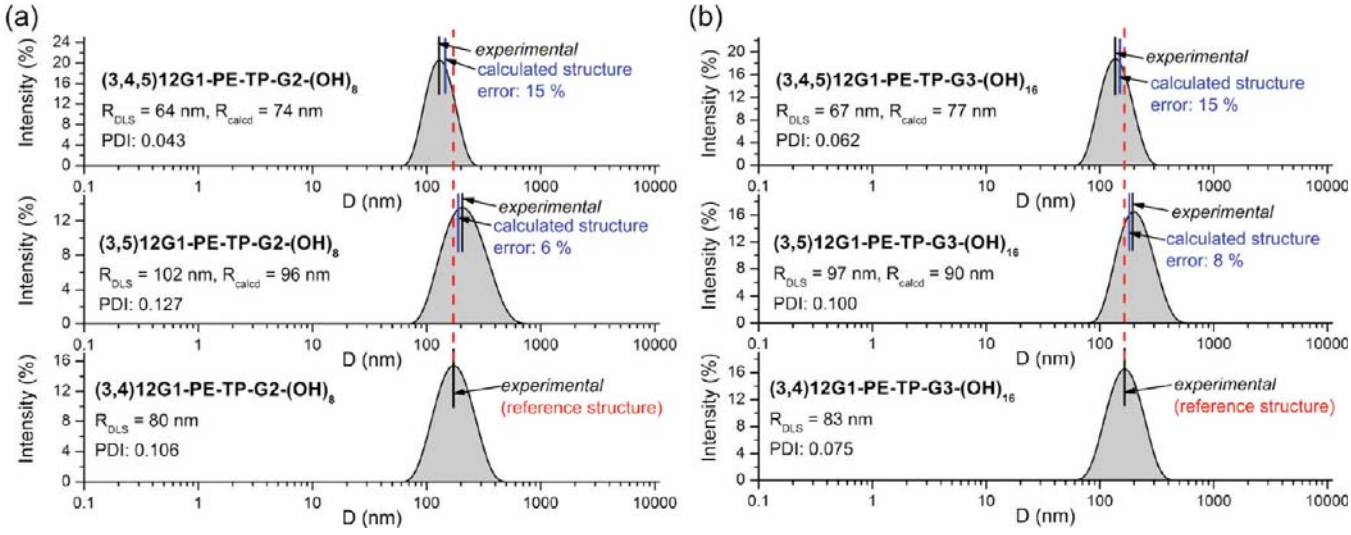

Figure 10. The plots of DLS intensity vs diameter (D) collected from the sublibrary of Janus-dendrimers Y-PE-TP-G2-$(OH)_8$ by injection from ethanol into water (a) and Y-PE-TP-G3-$(OH)_{16}$ by injection from tetrahydrofuran into water (b). The increase and decrease of the size of the vesicles as a function of the branching pattern of the dendrimer aliphatic region are illustrated by the vertical dashed red line. In all cases, the calculated D of the dendrimersome and its percentage deviation from the experimental value are indicated.

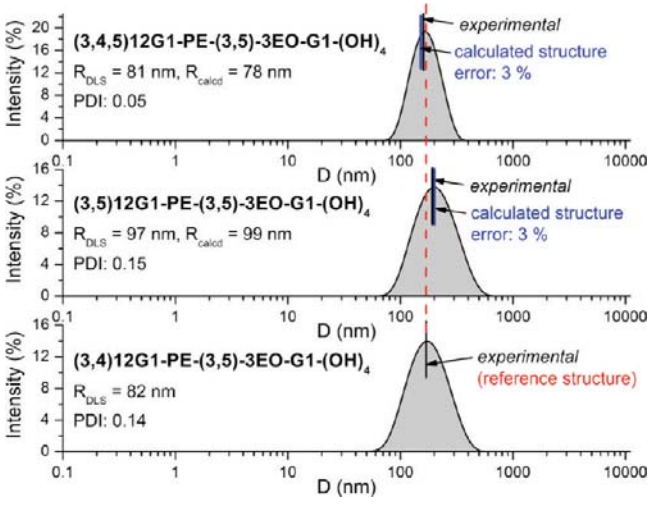

Figure 11. The plots of DLS intensity vs diameter (D) collected from the sublibrary of Janus-dendrimers Y-PE-(3,5)-3EO-G1-$(OH)_4$ by injection from tetrahydrofuran in water. The increase and decrease of the size of the vesicles as a function of the branching pattern of the dendrimer aliphatic region are illustrated by the vertical dashed red line. In all cases, the calculated D of the dendrimersome and its percentage deviation from the experimental value are indicated.

In eq 8, the ratio $M_{wt}^{\text{ref str}}/M_{wt}$ is a correction factor that accounts for the possibility that the molecular weight of Janus dendrimer for which the size of the self-assembled dendrimersome is predicted can differ from the molecular weight of the Janus dendrimer chosen as reference structure. The reference structure provides a mechanism to keep δ, Δ, and c values the same across sublibraries.

In the previous sections, it was established that there is a direct dependence between the branching pattern of the hydrophobic part of the amphiphilic Janus dendrimer and the size of the dendrimersome formed in water (Figures 2−4 and Table 2), as well as the layer thickness forming the lamellar phases in bulk (eqs 1 and 2, Supporting Tables ST1−ST5, and Figure 9). Therefore, eq 7 was applied to predict the size of all the dendrimersomes formed by Janus dendrimers that exhibited a lamellar phase upon their self-organization in bulk. Table 3 details the predicted size of the dendrimersome self-assembled in water from 21 Janus dendrimers. To minimize the effect of a different structure of the hydrophilic part of the Janus dendrimer to the size of the dendrimersomes formed in water, the calculations reported in Table 3 were performed by choosing one of the three Janus dendrimers (3,4)12G1-X, (3,5)12G1-X, and (3,4,5)12G1-X from each sublibrary as reference structure. Dendrimersomes were prepared by injection both from ethanol and THF solutions. However, the current solvent of choice for applications is ethanol. Therefore, although the size of the dendrimersomes obtained from the two solvents is to certain extent different, most probably due to the different conformations of the Janus dendrimers in the two solvents, the agreement between their experimental and calculated values is excellent in both solvents. These results supports the accuracy of this methodology.

For example, from the sublibrary 15, Y-PE-TP-G2-$(OH)_8$ with Y = {(3,4)12G1-, (3,5)12G1-, and (3,4,5)12G1-}, the (3,4)12G1-PE-TP-G2-$(OH)_8$ was chosen as reference structure. Note that the calculations of predicting the size of dendrimersomes are performed similarly if any of the other two Janus dendrimers from the sublibrary is selected as reference structure. The thickness of the wall of the dendrimersome self-assembled by injection in water from (3,4)12G1-PE-TP-G2-$(OH)_8$ is $d_{001}^{\text{ref str}} = 6.97$ nm (Table 3, Figure 9). The radii of dendrimersomes, determined experimentally by DLS, is $R_{DLS}^{\text{ref str}} = 79.5$ nm. As mentioned before, R_{DLS} may slightly overestimate the real size since R_{DLS} is calculated from the hydrodynamic radius. The thickness of the wall of dendrimersomes self-assembled by injection in water from (3,5)12G1-PE-TP-G2-$(OH)_8$ is $d_{001} = 4.59$ nm (Table 3, Figure 9). Using these three parameters, eq 7 gives the predicted radius of the dendrimersome self-assembled in water from (3,5)12G1-PE-TP-G2-$(OH)_8$, $R_{calcd} = 4.59/2 + (12 \times 4.59 \times \Delta - 3 \times 4.59^3)^{1/2}/(6 \times 4.59) = 96.0$ nm, where $\Delta = 79.5^3 - (79.5 - 6.97)^3 = 120\,908.5$ nm^3 (eq 8). The predicted

dx.doi.org/10.1021/ja208762u | J. Am. Chem. Soc. XXXX, XXX, 000–000

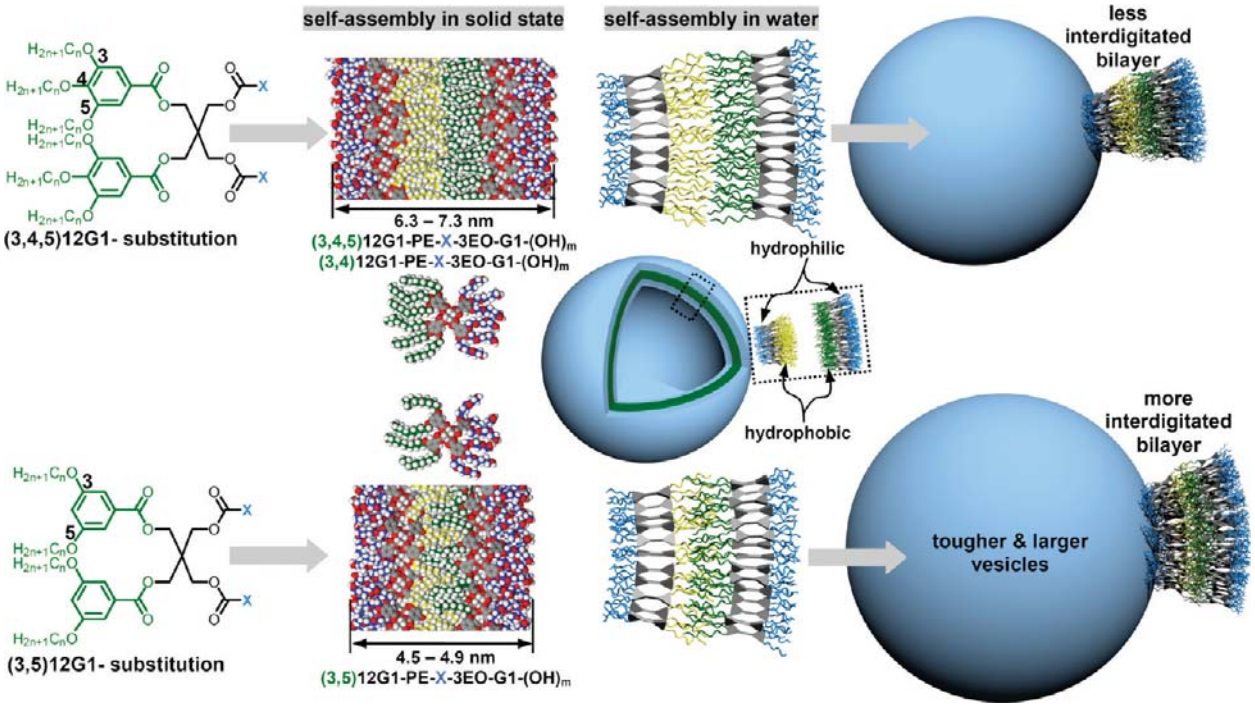

Figure 12. Schematic of the self-assembly of Janus-dendrimers into dendrimersomes. The alkyl substitution pattern controls the size and mechanical properties of the vesicle via the degree of interdigitation of the vesicle wall. The different degree of interdigitation of the hydrophobic part of the vesicle wall is generated by the tendency of the alkyl chains to achieve the same local packing density. For clarity, the alkyl chains of the inner and outer layer of Janus-dendrimers forming the vesicle shell are colored in yellow and green, respectively.

size of the dendrimersome self-assembled from (3,5)12G1-PE-TP-G2-$(OH)_8$ of 96.0 nm is remarkably close to the experimental value R_{DLS} = 102 nm. The deviation between the predicted and experimental values is only 6%.

The agreement between the experimental and predicted size of the dendrimersomes is illustrated in Figures 10 and 11, together with their corresponding DLS intensity versus D data. The representative DLS data shown in Figures 10 and 11 were collected from the indicated sublibraries of Janus dendrimers by injection from ethanol or from tetrahydrofuran. In all cases shown in Figures 10 and 11, the predicted size of the dendrimersomes is close to the experimental value, with a typical deviation of about 3−15%. Moreover, all the predicted values presented in Table 3 follow the expected correlation showing that R_{calcd} and R_{DLS} are either both larger, or both smaller than the radius of the dendrimersome chosen as reference structure, $R_{DLS}^{ref\ str}$.

The approximation that the thickness of the vesicle membrane is equal to the thickness of the layers forming the lamellar phases in bulk reported in Figures 2−4, d_{001}, excludes the hydration, solvation, and the hydrophobic effects and the possible tilted organization of the Janus-dendrimers in the lamellar phase. In situ X-ray diffraction preliminary experiments that monitored the hydration and dehydration of the lamellar phase formed by (3,4,5)12G1-PE-BMPA-G2-$(OH)_8$ revealed a typical change of d_{001} of at most 5%. Furthermore, it was shown that in bulk the hydrophilic part of the Janus-dendrimers forming lamellar phases can be interdigitated (Figures 5 and 6), whereas in water, the hydrophilic part of the vesicle wall is hydrated but not interdigitated. Therefore, the thickness of the vesicle membrane is expected to be comparable or larger than the d_{001} extracted from the XRD analysis. Nevertheless, in eqs 7 and 8 used to predict the size of the vesicles, in a first order of approximation the relative ratio of the vesicle wall thickness is more important. This explains why, even though this approximation might be considered too coarse, there is good agreement between the predicted and experimental vesicle size (Table 3, and Figures 9−11).

Figure 12 summarizes the inverse proportionality between the thickness of the vesicle wall, that is controlled by the molecular structure of the Janus-dendrimer, and the size and mechanical properties of the dendrimersomes.

CONCLUSIONS

The combined analysis of the self-assembly process of amphiphilic Janus dendrimers in bulk and in water demonstrated that the molecular structure of the dendrimer determines the morphology of the supramolecular assemblies. The results demonstrated that the self-assembly process in water follows pathways that preserve the surface curvature of the assemblies formed in bulk. A direct correlation between the branching pattern of the hydrophobic part of the Janus dendrimer and the thickness of the layers forming lamellar phases in bulk and of the vesicle wall was demonstrated.

Somewhat surprisingly, the statistical analysis of the size of the dendrimersomes prepared under identical conditions, formed by injection from alcohol into water, demonstrated that the vesicles with a thinner wall, self-assembled from amphiphilic Janus dendrimers with 3,5-bis(dodecyloxy)benzene hydrophobic groups, are larger than those with 3,4-bis(dodecyloxy)benzene and 3,4,5-tris(dodecyloxy)benzene. The theoretical fit of the experimental dependence between the size of the dendrimersome and concentration of Janus-dendrimers in water, c, provided a direct proportionality between the mass of the vesicle wall and c. This proportionality was exploited to develop a methodology to

dx.doi.org/10.1021/ja208762u | J. Am. Chem. Soc. XXXX, XXX, 000–000

predict the size of the vesicle. This methodology provided the size of dendrimersomes formed by 21 amphiphilic Janus dendrimers in good agreement with their experimental size determined from DLS data obtained for dendrimersomes generated by injection in water from a particular water miscible solvent. This analysis demonstrated that the dendrimersomes with thinner membrane are larger, tougher, and more stable due to the increased degree of interdigitation of the alkyl chains forming the hydrophobic part of the vesicle membrane. The clarification of the smaller difference between the 3,4- and 3,4,5-hydrophobic branching patterns requires additional experiments. The main weakness of this approach is that one still needs to fully characterize a reference structure for any given Janus dendrimer in order to predict the size of the dendrimersome.

■ ASSOCIATED CONTENT

Supporting Information. Experimental procedures with complete structural analysis and complete ref 3. This material is available free of charge via the Internet at http://pubs.acs.org.

■ AUTHOR INFORMATION

Corresponding Author
Percec@sas.upenn.edu

■ ACKNOWLEDGMENT

Financial support by the National Science Foundation (Grants DMR-1066116 and DMR-1120901) and by the P. Roy Vagelos Chair at the University of Pennsylvania is gratefully acknowledged.

■ REFERENCES

(1) (a) Bangham, A. D.; Standish, M. M.; Watkins, J. C. *J. Mol. Biol.* **1965**, *13*, 238–252. (b) Sessa, G.; Weissman., G. *J. Lipid Res.* **1968**, *9*, 310–318. (c) Lasic, D. D. *Nature* **1997**, *387*, 26–27. (d) Lasic, D. D. *Biochem. J.* **1988**, *256*, 1–11. (e) Guo, X.; Szoka, F. C., Jr. *Acc. Chem. Res.* **2003**, *36*, 335–341. (f) Elbayoumi, T. A.; Torchilin, V. P. *Methods Mol. Biol.* **2010**, *605*, 1–27.

(2) (a) Discher, B. M.; Won, Y. -Y.; Ege, D. S.; Lee, J. C.-M.; Bates, F. S.; Discher, D. E.; Hammer, D. A. *Science* **1999**, *284*, 1143–1146. (b) Discher, D. E.; Eisenberg, A. *Science* **2002**, *297*, 967–973. (c) Morishima, Y. *Angew. Chem., Int. Ed.* **2007**, *46*, 1370–1372. (d) Bellomo, E. G.; Wyrsta, M. D.; Pakstis, L.; Pochan, D. J.; Deming, T. J. *Nat. Mater.* **2004**, *3*, 244–248. (e) Kim, K. T.; Zhu, J.; Meeuwissen, S. A.; Cornelissen, J. J. L. M.; Pochan, D. J.; Nolte, R. J. M.; van Hest, J. C. M. *J. Am. Chem. Soc.* **2010**, *132*, 12522–12524. (f) Antonietti, M.; Förster, S. *Adv. Mater.* **2003**, *15*, 1323–1333. (g) Kita-Tokarczyk, K.; Meier, W. *Chimia* **2008**, *62*, 820–825. (h) Li, M.-H.; Keller, P. *Soft Matter* **2009**, *5*, 927–937. (i) Blanazs, A.; Armes, S. P.; Ryan, A. J. *Macromol. Rapid Commun.* **2009**, *30*, 267–277.

(3) Percec, V.; et al. *Science* **2010**, *328*, 1009–1014.

(4) (a) Singer, S. J.; Nicolson, G. L. *Science* **1972**, *175*, 720–731. (b) Hanczyc, M. M.; Szostak, J. W. *Curr. Opin. Chem. Biol.* **2004**, *8*, 660–664. (c) Luisi, P. L.; Walde, P.; Oberholzer, T. *Curr. Opin. Colloid Interface Sci.* **1999**, *4*, 33–39. (d) Schrum, J. P.; Zhu, T. F.; Szostak, J. W. *Cold Spring Harbor Perspect. Biol.* **2010**, *9*, a002212. (e) Haluska, C. K.; Riske, K. A.; Marchi-Artzner, V.; Lehn, J. M.; Lipowsky, R.; Dimova, R. *Proc. Natl. Acad. Sci. U.S.A.* **2006**, *103*, 15841–15846. (f) Tanner, P.; Egli, S.; Balasubramanian, V.; Onaca, O.; Palivan, C. G.; Meier, W. *FEBS Lett.* **2011**, *585*, 1699–1706.

(5) (a) Ghadiri, M. R.; Granja, J. R.; Buehler, L. K. *Nature* **1994**, *369*, 301–304. (b) Percec, V.; Dulcey, A. E.; Balagurusamy, V. S. K.; Miura, Y.; Smidrkal, J.; Peterca, M.; Nummelin, S.; Edlund, U.; Hudson, S. D.; Heiney, P. A.; Duan, H.; Magonov, S. N.; Vinogradov, S. A. *Nature* **2004**, *430*, 764–768. (c) Kumar, M.; Grzelakowski, M.; Zilles, J.; Clark, M.; Meier, W. *Proc. Natl. Acad. Sci. U.S.A.* **2007**, *104*, 20719–20724.

(6) Farokhzad, O. C.; Langer, R. *ACS Nano* **2009**, *3*, 16–20.

(7) (a) Barenholz, Y. *Curr. Opin. Colloid Interface Sci.* **2001**, *6*, 66–77. (b) Antimisiaris, S. G.; Kallinteri, P.; Fatouros, D. G. In *Pharmaceutical Manufacturing Handbook: Production and Processes.*; Gad, S. C., Ed.; Wiley: New York, 2008; pp 443−533. (c) Malam, Y.; Loizidou, M.; Seifalian, A. M. *Trends Pharmacol. Sci.* 2009, 30, 592−599. (d) Schroeder, A.; Turjeman, K.; Schroeder, J. E.; Leibergall, M.; Barenholz, Y. *Exp. Opin. Drug Delivery* **2010**, *7*, 1175–1189. (e) Allen, T. M.; Cullis, P. R. *Science* **2004**, *303*, 1818–1822. (f) Allen, T. M. *Nat. Rev. Cancer* **2002**, *2*, 750–763. (g) Lasic, D. D.; Templeton, N. S. *Adv. Drug Delivery Rev.* **1996**, *20*, 221–266.

(8) Picard, F. J.; Bergeron, M. G. *Drug Discovery Today* **2002**, *7*, 1092–1101.

(9) (a) Kulkarni, V. S. In *Delivery System Handbook for Personal Care and Cosmetic Products*; Rosen, M. R., Ed.; William Andrew, Inc.: East Norwich, NY, 2005; pp 285−302. (b) Chanchal, D.; Pharm, M.; Swarnlata, S.; Pharm, M. *J. Cosmet. Dermatol.* **2008**, *7*, 89–95. (c) Homann, H.-H.; Rosbach, O.; Moll, W.; Vogt, P. M.; Germann, G.; Hopp, M.; Langer-Brauburger, B.; Reimer, K.; Steinau, H.-U. *Ann. Plast. Surg.* **2007**, *59*, 423–427. (d) Taylor, T. M.; Davidson, P. M.; Bruce, B. D.; Weiss, J. *Crit. Rev. Food Sci. Nutr.* **2005**, *45*, 587–605. (e) Nohynek, G. J.; Lademann, J.; Ribaud, C.; Roberts, M. S. *Crit. Rev. Toxicol.* **2007**, *37*, 251–277.

(10) (a) Nagayasu, A.; Uchiyama, K.; Kiwada, H. *Adv. Drug Delivery Rev.* **1999**, *40*, 75–87. (b) Zhu, T. F.; Szostak, J. W. *PLoS One* **2009**, *4*, e5009.

(11) (a) Szoka, F., Jr.; Papahadjopoulos, D. *Annu. Rev. Biophys. Bioeng.* **1980**, *9*, 467–508. (b) Huang, C.-H. *Biochemistry* **1969**, *8*, 344–352. (c) Barenholz, Y.; Gibbes, D.; Litman, B. J.; Goll, J.; Thompson, T. E.; Carlson, F. D. *Biochemistry* **1977**, *16*, 2806–2810. (d) Szoka, F., Jr.; Papahadjopoulos, D. *Proc. Natl. Acad. Sci. U.S.A.* **1978**, *75*, 4194–4198. (e) Batzri, S.; Korn, E. D. *Biochim. Biophys. Acta* **1973**, *298*, 1015–1019. (f) Bridson, R. H.; Santos, R. C. D.; Al-Duri, B.; McAllister, S. M.; Robertson, J.; Alpar, H. O. *J. Pharm. Pharmacol.* **2006**, *58*, 775–785. (g) Frisken, B. J.; Asman, C.; Patty, P. J. *Langmuir* **2000**, *16*, 928–933.

(12) (a) Lasic, D. D. *Biochem. J.* **1988**, *256*, 1–11. (b) Adams, D. J.; Kitchen, C.; Adams, S.; Furzeland, S.; Atkins, D.; Schuetz, P.; Fernyhough, C. M.; Tzokova, N.; Ryan, A. J.; Butler, M. F. *Soft Matter* **2009**, *5*, 3086–3096. (c) Battaglia, G.; Ryan, A. J. *Nat. Mater.* **2005**, *4*, 869–876. (d) Luisi, P. L. *J. Chem. Educ.* **2001**, *78*, 380–384. (e) Joannic, R.; Auvray, L.; Lasic, D. D. *Phys. Rev. Lett.* **1997**, *78*, 3402–3405. (f) Kaler, E. W.; Murthy, A. K.; Rodriguez, B. E.; Zasadzinski, J. A. N. *Science* **1989**, *245*, 1371–1374. (g) Jung, H. T.; Coldren, B.; Zasadzinski, J. A.; Iampietro, D. J.; Kaler, E. W. *Proc. Natl. Acad. Sci. U.S.A.* **2001**, *98*, 1353–1357.

(13) Ruysschaert, T.; Germain, M.; da Silva Gomes, J. F. P.; Fournier, D.; Sukhorukos, G. B.; Meier, W.; Winterhalter, M. *IEEE Trans. Nanobiosci.* **2004**, *3*, 49–55.

(14) Ringsdorf, H.; Schlarb, B.; Venzmer, J. *Angew. Chem., Int. Ed. Engl.* **1988**, *27*, 113–158.

(15) Thomas, J. L.; Tirrell, D. A. *Acc. Chem. Res.* **1992**, *25*, 336–342.

(16) (a) Allen, T. M.; Chonn, A. *FEBS Lett.* **1987**, *223*, 42–46. (b) Allen, T. M. *Trends Pharmacol. Sci.* **1994**, *15*, 215–220. (c) Papahadjopoulos, D.; Allen, T. M.; Gabizon, A.; Mayhew, E.; Matthay, K.; Huang, S. K.; Lee, K.-D.; Woodle, M. C.; Lasic, D. D.; Redemann, C.; Martin, F. J. *Proc. Natl. Acad. Sci. U.S.A.* **1991**, *88*, 11460–11464. (d) Lasic, D. D. *Angew. Chem., Int. Ed. Engl.* **1994**, *33*, 1685–1698. (e) Lasic, D. D.; Needham, D. *Chem. Rev.* **1995**, *95*, 2601–2628.

(17) (a) Huang, Z.; Szoka, F. C., Jr. *J. Am. Chem. Soc.* **2008**, *130*, 15702–15712. (b) Huang, Z.; Jaafari, M. R.; Szoka, F. C., Jr. *Angew. Chem., Int. Ed.* **2009**, *48*, 4146–4149. (c) Foglia, F.; Barlow, D. J.; Szoka, F. C., Jr.; Huang, Z.; Rogers, S. E.; Lawrence, M. J. *Langmuir* **2011**, *27*, 8275–8281.

(18) (a) Rosen, B. M.; Wilson, C. J.; Wilson, D. A.; Peterca, M.; Imam, M. R.; Percec, V. *Chem. Rev.* **2009**, *109*, 6275–6540. (b) Al-Jamal,

K. T.; Ramaswamy, C.; Florence, A. T. *Adv. Drug Delivery Rev.* **2005**, *57*, 2238–2270. (c) Malik, N.; Wiwattanapatapee, R.; Klopsch, R.; Lorenz, K.; Frey, H.; Weener, J. W.; Meijer, E. W.; Paulus, W.; Duncan, R. *J. Controlled Release* **2000**, *65*, 133–148.

(19) (a) Esfand, R.; Tomalia, D. A. *Drug Discovery Today* **2001**, *6*, 427–436. (b) Gensch, T.; Tsuda, K.; Dol, G. C.; Latterini, L.; Weener, J. W.; Schenning, A. P. H. J.; Hofkens, J.; Meijer, E. W.; De Schryver, F. C. *Pure Appl. Chem.* **2001**, *73*, 435–441. (c) Svenson, S.; Tomalia, D. A. *Adv. Drug Deliverry Rev.* **2005**, *57*, 2106–2129. (d) Tomalia, D. A.; Reyna, L. A.; Svenson, S. *Biochem. Soc. Trans.* **2007**, *35*, 61–67. (e) Menjoge, A. R.; Kannan, R. M.; Tomalia, D. A. *Drug Discovery Today* **2010**, *15*, 171–185. (f) Gillies, E. R.; Fréchet, J. M. J. *Drug Discovery Today* **2005**, *10*, 35–43. (g) Lee, C. C.; MacKay, J. A.; Fréchet, J. M. J.; Szoka, F. C. *Nat. Biotechnol.* **2005**, *23*, 1517–1526. (h) Fox, M. E.; Szoka, F. C.; Fréchet, J. M. J. *Acc. Chem. Res.* **2009**, *42*, 1141–1151. (i) Majoros, I. J.; Williams, C. R.; Baker, J. R., Jr. *Curr. Top. Med. Chem.* **2008**, *8*, 1165–1179. (j) Tekade, R. K.; Kumar, P. V.; Jain, N. K. *Chem. Rev.* **2009**, *109*, 49–87. (k) Amir, R. J.; Pessah, N.; Shamis, M.; Shabat, D. *Angew. Chem., Int. Ed.* **2003**, *42*, 4494–4499. (l) Shamis, M.; Lode, H. N.; Shabat, D. *J. Am. Chem. Soc.* **2004**, *126*, 1726–1731. (m) Shabat, D. *J. Polym. Sci., Part A: Polym. Chem.* **2006**, *44*, 1569–1578. (n) van Donge, S. F. M.; De Hong, H.-P.; Peters, R. J. R. W.; Nallani, M.; Nolte, R. J. M.; van Hest, J. C. M. *Chem. Rev.* **2009**, *109*, 6212–6274. (o) Jain, N. K.; Asthana, A. *Expert Opin. Drug Delivery* **2007**, *4*, 495–512. (p) Mintzer, M. A.; Simanek, E. E. *Chem. Rev.* **2009**, *109*, 259–302.

(20) (a) Rosen, B. M.; Peterca, M.; Huang, C.; Zeng, X.; Ungar, G.; Percec, V. *Angew. Chem., Int. Ed.* **2010**, *49*, 7002–7005. (b) Peterca, M.; Imam, M. R.; Ahn, C.-H.; Balagurusamy, V. S. K.; Wilson, D. A.; Rosen, B. M.; Percec, V. *J. Am. Chem. Soc.* **2011**, *133*, 2311–2328.

(21) (a) Cho, B. K.; Jain, A.; Gruner, S. M.; Wiesner, U. *Science* **2004**, *305*, 1598–1601. (b) Bury, I.; Heinrich, B.; Bourgogne, C.; Guillon, D.; Donnio, B. *Chem.—Eur. J.* **2006**, *12*, 8396–8413. (c) Balagurusamy, V. S. K.; Ungar, G.; Percec, V.; Johansson, G. *J. Am. Chem. Soc.* **1997**, *119*, 1539–1555. (d) Percec, V.; Peterca, M.; Dulcey, A. E.; Imam, M. R.; Hudson, S. D.; Nummelin, S.; Adelman, P.; Heiney, P. A. *J. Am. Chem. Soc.* **2008**, *130*, 13079–13094.

(22) (a) Alam, M. A.; Motoyanagi, J.; Yamamoto, Y.; Fukushima, T.; Kim, J.; Kato, K.; Takata, M.; Saeki, A.; Seki, S.; Tagawa, S.; Aida, T. *J. Am. Chem. Soc.* **2009**, *131*, 17722–17723. (b) Choi, J. W.; Ryu, M. H.; Lee, E.; Cho, B. K. *Chem.—Eur. J.* **2010**, *16*, 9006–9009.

(23) Ungar, G.; Liu, Y. S.; Zeng, X. B.; Percec, V.; Cho, W. D. *Science* **2003**, *299*, 1208–1211.

(24) Zeng, X. B.; Ungar, G.; Liu, Y. S.; Percec, V.; Dulcey, A. E.; Hobbs, J. K. *Nature* **2004**, *428*, 157–160.

(25) Peterca, M.; Imam, M. R.; Leowanawat, P.; Rosen, B. M.; Wilson, D. A.; Wilson, C. J.; Zeng, X. B.; Ungar, G.; Heiney, P. A.; Percec, V. *J. Am. Chem. Soc.* **2010**, *132*, 11288–11305.

(26) (a) Falvey, P.; Lim, C. W.; Darcy, R.; Revermann, T.; Karst, U.; Giesbers, M.; Marcelis, A. T. M.; Lazar, A.; Coleman, A. W.; Reinhoudt, D. N.; Ravoo, B. J. *Chem.—Eur. J.* **2005**, *11*, 1171–1180. (b) Battaglia, G.; Ryan, A. J. *J. Am. Chem. Soc.* **2005**, *127*, 8757–8764. (c) Keg, P.; Lohani, A.; Fichou, D.; Lam, Y. M.; Wu, Y. L.; Ong, B. S.; Mhaisalkar, S. G. *Macromol. Rapid Commun.* **2008**, *29*, 1197–1202.

(27) (a) Seifert, U. *Adv. Phys.* **1997**, *46*, 13–137. (b) Safran, S. A.; Pincus, P.; Andelman, D. *Science* **1990**, *248*, 354–356. (c) Segota, S.; Tezak, D. *Adv. Colloid Interface Sci.* **2006**, *121*, 51–75.

(28) (a) Rawicz, W.; Olbrich, K. C.; McIntosh, T.; Needham, D.; Evans, E. *Biophys. J.* **2000**, *79*, 328–339. (b) Ma, L.; Eisenberg, A. *Langmuir* **2009**, *25*, 13730–13736.

(29) Olbrich, K.; Rawicz, W.; Needham, D.; Evans, E. *Biophys. J.* **2000**, *79*, 321–327.

(30) Bermudez, H.; Brannan, A. K.; Hammer, D. A.; Bates, F. S.; Discher, D. E. *Macromolecules* **2002**, *35*, 8203–8208.

(31) Paula, S.; Volkov, A. G.; VanHoek, A. N.; Haines, T. H.; Deamer, D. W. *Biophys. J.* **1996**, *70*, 339–348.

(32) Lingwood, D.; Simons, K. *Science* **2010**, *327*, 46–50.

(33) (a) Liu, X. Y.; Wu, J.; Kim, J. S.; Eisenberg, A. *Langmuir* **2006**, *22*, 419–424. (b) Claessens, M.; Leermakers, F. A. M.; Hoekstra, F. A.; Stuart, M. A. C. *Langmuir* **2007**, *23*, 6315–6320. (c) Anraku, Y.; Kishimura, A.; Oba, M.; Yamasaki, Y.; Kataoka, K. *J. Am. Chem. Soc.* **2010**, *132*, 1631–1636.